Journal of proteome research

Article

pubs.acs.org/jpr

Secretome Analysis of Lipid-Induced Insulin Resistance in Skeletal Muscle Cells by a Combined Experimental and Bioinformatics Workflow

Atul S. Deshmukh,[†,‡] Juergen Cox,[†] Lars Juhl Jensen,[‡] Felix Meissner,[†] and Matthias Mann*[,†,‡]

[†]Department of Proteomics and Signal Transduction, Max-Planck-Institute of Biochemistry, Am Klopferspitz 18, D-82152 Martinsried, Germany

[‡]The Novo Nordisk Foundation Center for Protein Research, Faculty of Health and Medical Sciences, University of Copenhagen, Blegdamsvej 3B, Building 6.1, DK-2200 Copenhagen, Denmark

Supporting Information

ABSTRACT: Skeletal muscle has emerged as an important secretory organ that produces so-called myokines, regulating energy metabolism via autocrine, paracrine, and endocrine actions; however, the nature and extent of the muscle secretome has not been fully elucidated. Mass spectrometry (MS)-based proteomics, in principle, allows an unbiased and comprehensive analysis of cellular secretomes; however, the distinction of bona fide secreted proteins from proteins released upon lysis of a small fraction of dying cells remains challenging. Here we applied highly sensitive MS and streamlined bioinformatics to analyze the secretome of lipid-induced insulin-resistant skeletal muscle cells. Our workflow identified 1073 putative secreted proteins including 32 growth factors, 25 cytokines, and 29 metalloproteinases. In addition to previously reported proteins, we report hundreds of novel ones. Intriguingly, ~40% of the secreted proteins were regulated under insulin-resistant conditions, including a protein family with signal peptide and EGF-like domain structure that had not yet been associated with insulin resistance. Finally, we report that secretion of IGF and IGF-binding proteins was down-regulated under insulin-resistant conditions. Our study demonstrates an efficient combined experimental and bioinformatics workflow to identify putative secreted proteins from insulin-resistant skeletal muscle cells, which could easily be adapted to other cellular models.

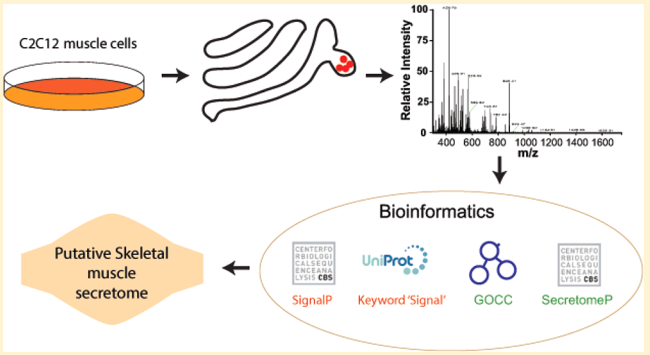

KEYWORDS: *myokines, quantitative proteomics, mass spectrometry, metabolism, glucose uptake, insulin signaling, diabetes, obesity, secretome, palmitic acid*

INTRODUCTION

Skeletal muscle is the primary tissue for insulin-mediated glucose uptake, accounting for up to 75% of the insulin-dependent glucose disposal.[1] Accordingly, insulin resistance in skeletal muscle plays a central role in the development of type 2 diabetes.[2] The role of inflammation in the pathogenesis of type 2 diabetes, obesity, and associated complications is now well established.[3] Pro-inflammatory proteins, such as tumor necrosis factor alpha (Tnf-α), interleukin 6 (Il-6), Il-1b, and monocyte chemotactic proteins 1 (Mcp-1), are elevated in experimental animal model of obesity and in obese humans.[4,5] Many of these pro-inflammatory proteins are secreted from adipose tissues.[6] In the last years, skeletal muscle has also been recognized as an important secretory organ. Proteins secreted from the contracting (exercised) skeletal muscle can possess anti-inflammatory properties and protect the body from chronic diseases such as type 2 diabetes.[7] Additionally, physical inactivity is associated with increased risk of type 2 diabetes,[8] which could hint at a potential role for secreted proteins from skeletal muscle in type 2 diabetes. Proteins and peptides that are secreted by skeletal muscles are often termed as myokines.[7] Given that muscle is the largest organ in the body, analysis of its secretome provides a basis for understanding how this tissue communicates with other organs such as adipose tissue, liver, pancreas, bone, and brain.

Proteomics based on high-resolution mass spectrometry (MS) has become a powerful tool for the analysis of protein abundance, modifications, and interactions.[9] For the investigation of cellular communication, proteomic analysis of secreted proteins holds enormous promise; however, secretome analysis faces several challenges, including the detection of bona fide secreted proteins at low concentrations by MS (pg/mL) and the separation of authentic secreted proteins from proteins derived from cell leakage or serum. We have recently shown that with current technology quantitative MS-based secretome

Received: July 31, 2015
Published: October 12, 2015

DOI: 10.1021/acs.jproteome.5b00720
J. Proteome Res. 2015, 14, 4885−4895

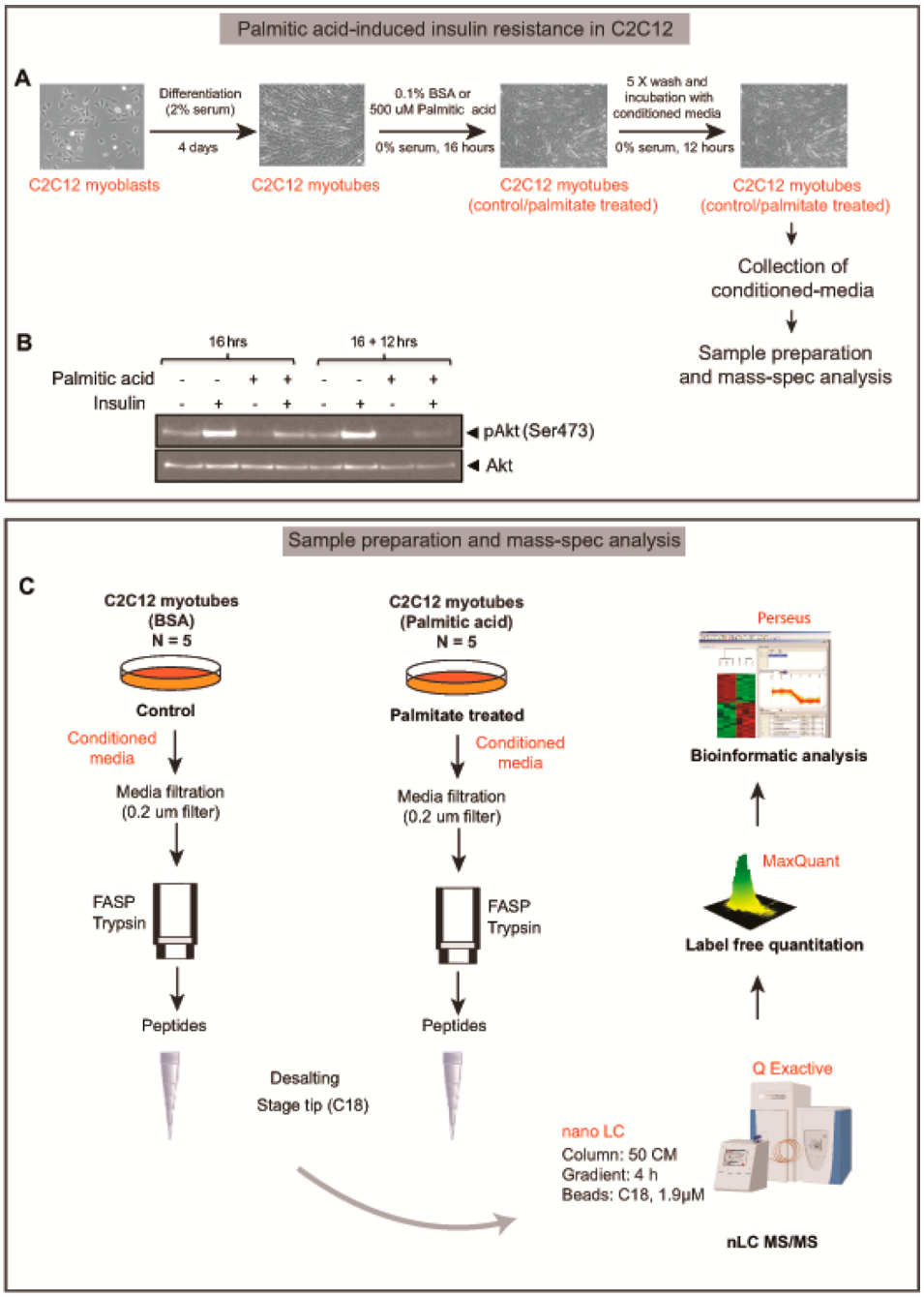

Figure 1. Proteomics analysis of lipid-induced insulin-resistant cells. (A) Differentiated C2C12 cells were treated with 500 μM palmitic acid in the presence of BSA (PA/BSA) for 16 h. Controls cells were treated with BSA. Conditioned media from PA/BSA treated cells were collected after 12 h of incubation in serum-free media. Proteomics analysis was performed on conditioned media and cell lysates. (B) Western blot analysis displaying impairment of insulin-stimulated Akt (Ser473) phosphorylation in PA/BSA-treated muscle cells. (C) Proteomics workflow of conditioned media from control and palmitate-treated insulin-resistant muscle cells. Proteins from conditioned media were digested on FASP filters. Peptides were eluted and analyzed by LC−MS on Q Exactive mass spectrometer.

analysis of immune cells can be performed with picogram sensitivity.[10] Bioinformatics approaches have been used to separate secreted proteins from nonsecreted proteins.[11] So far, these have typically been based either on algorithms that predict signal peptides from primary sequence or on subcellular locations from curated databases or on a combination of both. Because proteins may carry out different functions in different cellular locations,[12] it is inherently difficult to discriminate secreted proteins from nonsecreted ones. Thus, despite the technical advances in mass spectrometry and sample preparation, the bioinformatics analysis and interpretation of the data remains a challenge.

Proteomic profiling of the conditioned media from mouse, rat, and human skeletal muscle cells has already helped to identify hundreds of secreted proteins.[13−18] One such study reported that insulin stimulation alters the secretome profile of skeletal muscle cells, which would suggest that the protein secretion profile of skeletal muscle may differ between insulin resistance states.[15] Despite these pioneering studies, the

DOI: 10.1021/acs.jproteome.5b00720
J. Proteome Res. 2015, 14, 4885−4895

secretomes of skeletal muscle cells in the insulin sensitive or resistant states have not been fully characterized.

Insulin resistance precedes the diagnosis of type 2 diabetes.[19] Lipid-induced insulin resistance has been linked to multiple cellular events including accumulation of ceramides,[20] impaired insulin-stimulated phosphatidylinositol 3-kinase activity,[21] activation of protein kinase C ζ,[22] mitochondrial dysfunction,[23] and activation of nuclear factor κB (NF-κB).[24] Moreover, increased levels of plasma FFA contribute to impaired insulin signaling, leading to reduced insulin sensitivity and glucose uptake in insulin-sensitive tissues.[19,25,26]

Here we performed a proteomic analysis of the conditioned media from C2C12 myotubes, which are muscle cells that are differentiated into muscle fibers. Treating these myotubes with palmitic acid constitutes a frequently used model of induced insulin resistance.[20,21] In this study, we sought to develop a stringent bioinformatics workflow to help characterize the skeletal muscle secretome and to identify novel myokines, especially those whose secretion is modulated under lipid-induced insulin resistance conditions.

EXPERIMENTAL PROCEDURES

Cell Culture

C2C12 cells (myoblasts) were grown in Eagle's minimum essential medium supplemented with 2 mM L-glutamine and 10% fetal bovine serum (FBS) plus antibiotics in a humidified atmosphere with 5% CO2 in air. Undifferentiated myoblasts were grown to confluence in normal growth media. To induce differentiation, the amount of serum in the media was reduced to 2%. Cells were differentiated for 4 days. Growth medium was replaced with fresh medium every 2 days over a period of 4 days. Throughout the experiment, cells were grown on 10 cm plates with 10 mL of growth/differentiation medium.

Fatty Acid Treatment

Palmitic acid was conjugated with BSA at 2:1 molar ratio. After 4 days of differentiation, C2C12 myotubes were treated with 0.5 mM palmitic acid (Sigma-Aldrich) or 0.1% fatty acid free Bovine Serum Albumin (BSA) (Sigma-Aldrich) for 16 h. Because the cell culture media in this stage of the experiment contained high concentration of BSA, it was not suitable for the proteomic analysis. Therefore, cells were washed five times with serum-free media (conditioned media) to reduce the amount of contaminating BSA and incubated for another 12 h in the conditioned media. Finally, we collected the conditioned media for proteomic analysis. This procedure was performed in quintuplicate (biological replicates) for palmitic acid/BSA-treated cells. We term BSA-treated samples "control" and palmitic-acid-treated cell "palmitate-treated". Viability of cells before, during, and after palmitic acid/BSA treatment was monitored using the Trypan blue exclusion technique. After post-treatment with BSA or palmitic acid, we observed <10% cell death.

Palmitic-Acid-Induced Insulin Resistance

To examine palmitic-acid-induced insulin resistance, C2C12 myotubes were treated with 100 nM of insulin (Sigma-Aldrich) for 10 min. Cells were treated with insulin immediately after 16 h of palmitic acid treatment as well as 12 h of post treatment (Figure 1A). Cells were harvested and lysed in buffer containing 0.1 M Tris-HCl, pH 7.5, 0.1 M DTT, and 4% SDS. Cell lysates (20 μg of proteins) were separated on SDS-PAGE. Insulin-induced Akt (Ser473) phosphorylation was measured by immunoblotting (phospho-Akt (Ser473), Cell Signaling Technology). Palmitic-acid-induced insulin resistance was confirmed by impaired Akt (Ser473) phosphorylation under insulin-stimulated conditions (Figure 1B).

Sample Preparation for Proteomic Analysis

Proteomic analysis was performed on the conditioned media from BSA- and palmitic acid-treated cells. Conditioned media collected after 12 h postpalmitic acid/BSA treatment were centrifuged and filtered using 0.2 μm filter (Millipore) to ensure removal of any dead cells. Enzymatic digestion was performed on the proteins secreted in the media. To 500 μL of conditioned media, 60 mg of urea, 16 μL of 1 M DTT, and 5 μL of 1 M HEPES were added and mixed, and samples were incubated at 56 °C for 15 min. Thereafter samples were transferred to an Ultracel YM-10 10,000 molecular weight cutoff centrifugal filter (Millipore), spun down, and washed two times with 200 μL of 2 M urea in 0.1 M Tris/HCl pH 8.5. Proteins were alkylated with 55 mM iodoacetamide for 30 min in the dark. Filters were washed two times with 2 M urea in 0.1 M Tris/HCl pH 8. After the final wash, 100 μL of 2 M urea (pH 8) was added on the filters. Subsequently proteins were digested with 0.5 μg LysC (Wako) for 3 h at room temperature and 0.5 μg trypsin (Promega, Manheim, Germany) for 16 h at 37 °C.

To measure the cellular proteome from the same cells that we had measured the secretomes of, we lysed differentiated C2C12 cells in buffer consisting of 0.1 M Tris-HCl, pH 7.5, 0.1 M DTT, and 4% SDS and incubated at 95 °C for 5 min. Lysates were sonicated using a Branson-type sonicator and were then clarified by centrifugation at 16 000g for 10 min. Cell lysates were diluted in 8 M urea in 0.1 M Tris-HCl, followed by protein digestion with trypsin according to the FASP protocol.[27] After an overnight digestion, peptides were eluted from the filters with 25 mM ammonium bicarbonate buffer. Peptides were recovered by centrifugation, acidified with 0.5% trifluoroacetic acid, and desalted on reverse-phase C18 StageTips.[28] Peptides were eluted using 20 μL of 80% acetonitrile in 0.5% acetic acid. The volume was reduced in a SpeedVac and the peptides were resuspended in buffer containing 2% acetonitrile and 0.1% formic acid.

LC–MS/MS Analysis

The peptides were analyzed using LC–MS instrumentation consisting of an Easy nanoflow UHPLC (Thermo Fisher Scientific) coupled via a nanoelectrospray ion source (Thermo Fisher Scientific) to Q Exactive[29] mass spectrometer (Thermo Fisher Scientific). Peptides were separated on 50 cm column with 75 μm inner diameter packed in-house with ReproSil-Pur C18-aq 1.9 μm resin (Dr. Maisch). Peptides were loaded in buffer containing 0.5% formic acid and eluted with a 270 min linear gradient with buffer containing 80% acetonitrile and 0.5% formic acid (v/v) at 250 nL/min. Chromatography and column oven (Sonation) temperature were controlled and monitored in real time using SprayQC.[30] Mass spectra were acquired in a data-dependent manner, with an automatic switch between MS and MS/MS using a top 10 method. MS spectra were acquired in the Orbitrap analyzer with a mass range of 300–1750 m/z and 70 000 resolution at m/z 200. HCD peptide fragments were acquired with normalized collision energy of 25. The maximum ion injection times for the survey scan and the MS/MS scans were 20 and 60 ms, and the ion target values were set to 3e6 and 1e6, respectively. Data were acquired using Xcalibur software.

DOI: 10.1021/acs.jproteome.5b00720
J. Proteome Res. 2015, 14, 4885–4895

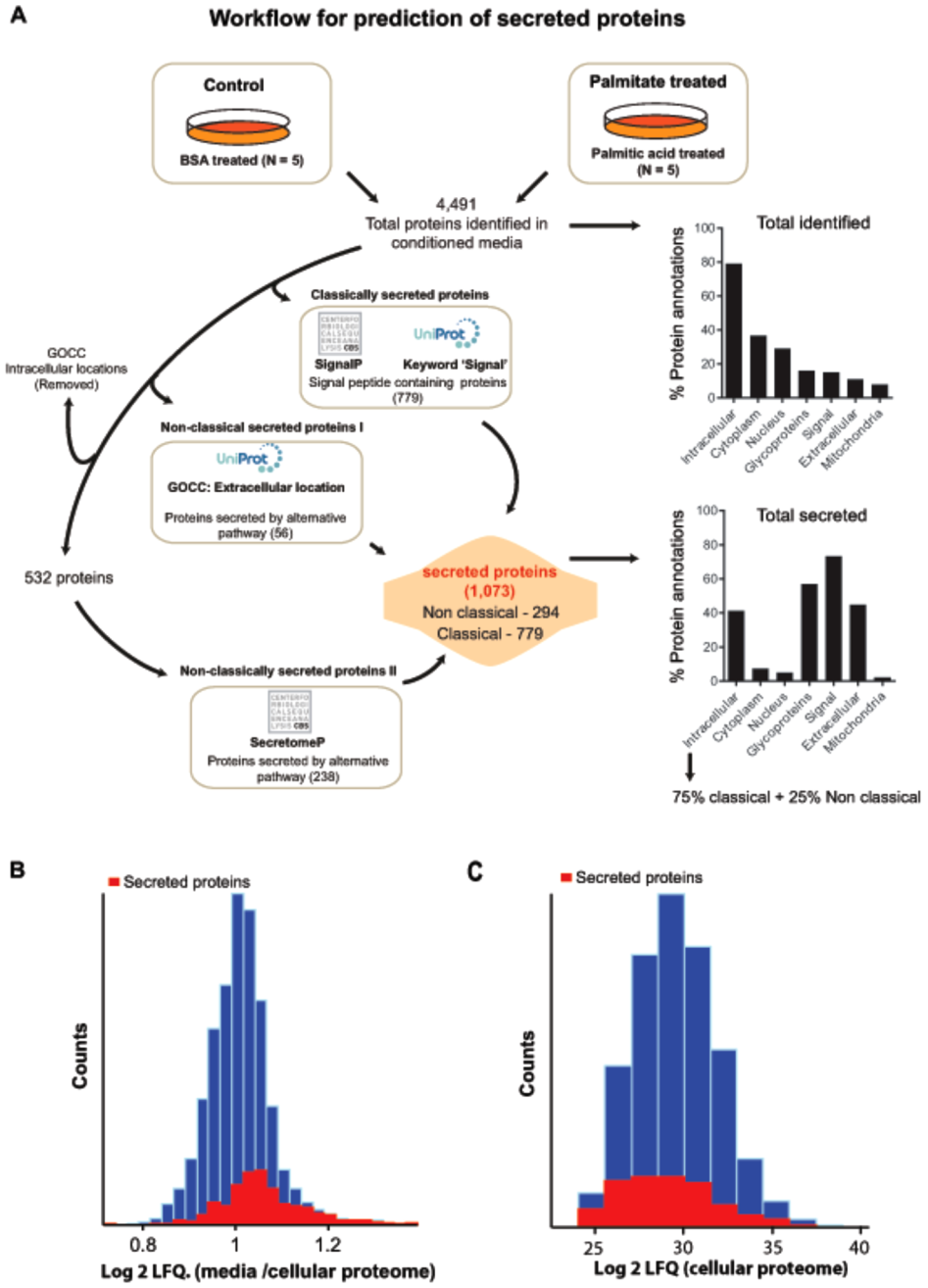

Figure 2. Bioinformatics workflow for the prediction of secreted proteins. (A) Using different bioinformatics tools, total identified proteins in conditioned media are separated into "classically secreted" and "nonclassically secreted proteins". Bar graph displays % proteins annotation for proteins detected in the conditioned media (top panel) and for the proteins that were classified as secreted proteins (bottom panel). (B) Histogram displaying the ratio of protein abundance (LFQ intensities) between proteins quantified in the media and proteins from cellular proteome of the muscle cells. Red bar shows the proteins which were predicted as secreted proteins. (C) Histogram displaying the distribution of protein abundances (LFQ intensities) from cellular proteomes. Red bar indicates the number of proteins we defined as secreted.

Computational MS Data Analysis

Mass spectra were analyzed using MaxQuant[31] (version 1.4.1.14) with the Adromeda search engine.[29] The initial maximum allowed mass deviation was set to 6 ppm for monoisotopic precursor ions and 20 ppm for MS/MS peaks. Enzyme specificity was set to trypsin, defined as C-terminal to arginine and lysine excluding proline, and a maximum of two missed cleavages were allowed. A minimal peptide length of six amino acids was required. Cabamidomethylcysteine was set as a fixed modification, while N-terminal acetylation and methionine oxidation were set as variable modifications. The spectra were searched by the Andromeda search engine against the mouse UniProt sequence database combined with 248 common contaminants and concatenated with the reversed versions of all sequences. The false discovery rate (FDR) was set to 1% for peptide and protein identifications. To match the identifications across different LC−MS runs, the "match between runs" option in MaxQuant was enabled with a retention time window of 30 s. In the case of identified peptides that were shared between two or more proteins, these were combined and reported in protein group. Contaminants and reverse identification were removed from further data analysis.

DOI: 10.1021/acs.jproteome.5b00720
J. Proteome Res. 2015, 14, 4885−4895

All statistical analyses of the MaxQuant output were performed with the Perseus program, which is part of MaxQuant (http://141.61.102.17/perseus_doku/doku.php?id=start, version 1.4.2.31). We used Gene Ontology (GO) biological process (GOBP), molecular function (GOMF), cellular component (GOCC), and UniProt Keywords to assign categorical annotations to identified proteins. Pfam database (http://pfam.xfam.org/) was used for the domain predictions.

Bioinformatics Workflow for the Prediction of Putative Secreted Proteins

Secreted proteins were filtered using a combination of the SignalP 4.1[32] and SecretomeP 2.0[33] prediction methods and UniProt keyword annotations—"Signal". SignalP predicts N-terminal signal peptides, whereas SecretomeP predicts secretory proteins following nonclassical, signal peptide-independent mechanisms. Default NN-score and D-score cut-offs were used for SecretomeP and SignalP, respectively. On the basis of these predictions, we selected the putative secreted proteins in three steps (Figure 2A). (1) From the total of the identified proteins, those with predicted signal peptides were extracted using SignalP and UniProt keyword annotation "Signal". These proteins were grouped as "classically" secreted proteins. (2) The remaining proteins were annotated with GO Cellular Component (GOCC). The proteins with "extracellular locations" were classified as "nonclassically secreted proteins - I". (3) From the remaining candidates, those annotated with "intracellular locations" (GOCC) were discarded. Protein sequences for the remaining proteins were analyzed with SecretomeP.[33] The proteins with SecretomeP NN-score >0.5 were grouped as "nonclassically secreted proteins II". Finally, the nonclassically secreted proteins-I and -II were grouped together as the proteins secreted by alternate pathways (nonclassical).

Statistical Analysis

Protein quantification in MaxQuant was performed using the built-in label-free quantification algorithm.[34] The proteins with at least three valid values in at least one group (control/palmitate treated) were considered as quantified. The data were imputed to fill missing data points by creating a Gaussian distribution of random numbers with a standard deviation of 30% in comparison with the standard deviation of measured values, and one standard deviation down-shifted from the mean to simulate the distribution of low signal values. Two sample *t* tests were performed on control and palmitate-treated group with FDR = 5% and S0 correction of 0.1.[35] Fischer's exact test was performed for the enrichment in the set of significantly changing proteins of GO annotations, UniProt keyword annotations, and Pfam domains, using Benjamini–Hochberg correction with an FDR cutoff of 5%.

RESULTS AND DISCUSSION

Palmitic Acid-Induced Insulin Resistance in C2C12 Muscle Cells

Akt plays an important role in insulin-mediated glucose uptake and glycogen synthesis;[36] hence its dysregulation is likely to impact glucose homeostasis. Among the free fatty acids (FFAs), palmitic acid is well-established for eliciting insulin resistance in previously insulin-sensitive cells including skeletal muscle cells.[20,22,24] Using this model, we induced insulin resistance in C2C12 myotubes (Figure 1). Palmitic-acid-induced insulin resistance can be monitored by suppression of insulin-stimulated glucose uptake, PI3K activity, or Akt (Ser473) phosphorylation.[20,22] Accordingly, we confirmed insulin resistance by measuring insulin-stimulated Akt (Ser473) phosphorylation. As expected, insulin robustly increased Akt (Ser473) phosphorylation in control (BSA) condition, while it failed to do so after palmitic acid treatment (Figure 1B). Because the secretome of C2C12 myotubes was measured 12 h postpalmitic acid treatment, we also confirmed that the cells were insulin-resistant at that time point (Figure 1B). We monitored the viability of cells before, during, and after palmitic acid/BSA treatment using the Trypan Blue exclusion technique. Under all conditions Tryphan-Blue-positive cells were below 10%, indicating that cells remained viable.

Secretome Analysis of C2C12 Muscle Cells

With high-resolution MS[29] and automated computational analysis in MaxQuant,[34] we detected 4491 protein groups in the conditioned media from the control and the palmitate-treated C2C12 myotubes together (Supplemental Table 1) (Figure 2A). In order to reduce the number and amount of background proteins in the conditioned medium, we omitted supplementation of serum proteins to the culture medium in the later stages, and this did not cause a reduction in viability (see above).

Secretomes contain the proteins released through the classical ER–Golgi pathways (classically secreted proteins), extracellular domains of plasma membrane proteins generated by protease shedding, and proteins secreted through different nonclassical pathways (nonclassically secreted proteins).[37] Our understanding of the secretome is constantly evolving as more and more proteins with multiple annotations are described as secreted proteins. One of the largest challenges in secretome analysis is to distinguish bona fide secreted proteins from the proteins that are released into the cell culture medium upon lysis of a small fraction of dying cells. In our data set, 15 and 11% of detected proteins were annotated in UniProt with the keywords "Signal" and in GOCC as "Extracellular", respectively (Figure 2A). We next searched for proteins containing features of known secreted proteins using both Gene Ontology annotation information and sequence-based prediction methods, SignalP[32] and SecretomeP.[33] On the basis of our streamlined computational workflow (experimental procedures), we identified 1073 putative secreted proteins from C2C12 cells, including classically and nonclassically secreted proteins as described later and in the experimental procedures (Figure 2A) (Supplemental Table 2). Among these are a wide variety of known secreted proteins such as growth factors (Fgf21, Igf1, Tgfb1, Bdnf), cytokines (Il34), chemokines (Ccl9, Cxcl1), and metalloproteinases (Nrd1, Mmp2, Bmp1). The secretome of C2C12 myotubes presented here is measured over a period of 12 h. Therefore, some of the secreted proteins might have been taken up again by the cells, and the real amount of secreted proteins may have been somewhat underestimated. The list of the putative secreted proteins in this study represents the largest muscle secretome (myokinome) so far. Notably, almost half of these proteins had not been identified in conditioned media from skeletal muscle before. A previous study reported the identification of 635 secreted proteins during the C2C12 myogensis program.[18] Despite our different experimental setup, we identified ~60% these proteins in our secreted protein data set (Figure S1A). A total of 80% of the secreted proteins from the current study were also identified our recent adult mouse skeletal muscle

DOI: 10.1021/acs.jproteome.5b00720
J. Proteome Res. 2015, 14, 4885–4895

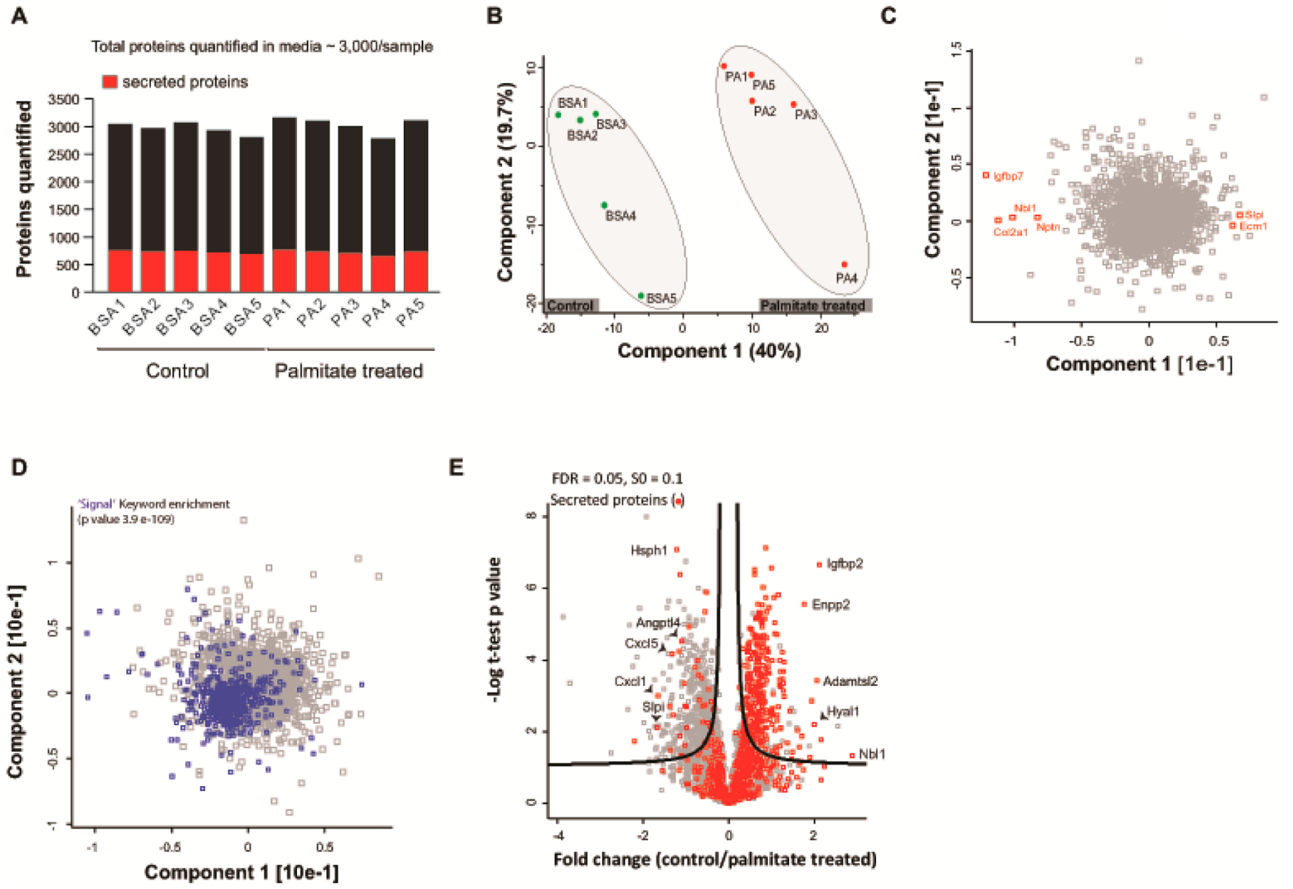

Figure 3. Comparative analysis of secretomes from control and palmitate-treated insulin resistant muscle cells. (A) Total number of quantified proteins in each sample. Red color represents the number of quantified secreted proteins. (B) PCA analysis of secretome from control and palmitate-treated insulin-resistant cells. (C) PCA loading for samples displayed in panel B. (D) Protein-category-based enrichment for samples displayed in panel B. (E) Volcano plot after two-sample *t* test for proteins detected in the media from control versus insulin resistant muscle cells. Red squares indicate proteins we defined as secreted.

proteome study,[38] indicating that the myokinome reported here is not restricted to our cellular model (Figure S1B). At the same time, we acknowledge limitations of the results acquired from C2C12 myotube model. For instance, the systemic components controlling homeostatic regulation in vivo are missing in cell cultures; the cellular metabolism may be more constant in vitro than in vivo and may therefore not be as representative.

The majority of known secreted proteins, regardless of their subsequent fate, are targeted for translocation across the endoplasmic reticulum membrane by an N-terminal signal peptide sequence and subsequently secreted through the classical secretion pathway. Often these proteins are secreted in low concentration and are heavily postranslationally modified, making their MS-based detection more difficult. Additionally, cell culture media are rich in salts and other compounds that can interfere with the proteomics analysis. Despite these challenges, our proteomic workflow enabled accurate quantitation of hundreds of classically secreted proteins. For instance, the small protein bone-derived neurotropic factor (Bdnf), which is known to be present in ng/mL concentrations in healthy human plasma,[39] was identified with three unique peptides (Supplemental Table 2, Figure S2C). Bdnf is produced by contracting skeletal muscle and regulates skeletal muscle lipid metabolism.[40] In our data set, 779 proteins were defined as classically secreted proteins (Figure 2A), supporting a pivotal role for skeletal muscle in interorgan communication.

Nonclassical secretion of proteins via the ER/Golgi-independent pathways is poorly understood. Because nonclassically secreted proteins by definition do not contain a signal peptide sequence and comprise proteins with various mechanistically distinct secretion paths,[37] their prediction is more difficult than that of classically secreted proteins. Among the tools available, SecretomeP is by far the most frequently used.[33] Instead of using SecretomeP on the complete data set of proteins identified in the supernatants, we used annotations to eliminate unnecessary false negatives and likely false positives. We achieved the former by filtering the proteins with the GOCC annotations indicating extracellular locations and categorized them as "nonclassical I" (56 proteins) (Figure 2A). This list includes several proteins, which have been reported to be secreted such as Annexins (Anxa1, Anxa A5) and high mobility group proteins (Hmgb1, Hmgb B2) (Supplemental Table 2).[41,42] We then removed the proteins with GOCC annotations indicating intracellular locations, which if predicted to be secreted would likely be false-positive predictions. The remaining proteins were run through SecretomeP, which yielded a second group of potentially nonclassically secreted proteins (nonclassical II, 238 proteins,

DOI: 10.1021/acs.jproteome.5b00720
J. Proteome Res. 2015, 14, 4885−4895

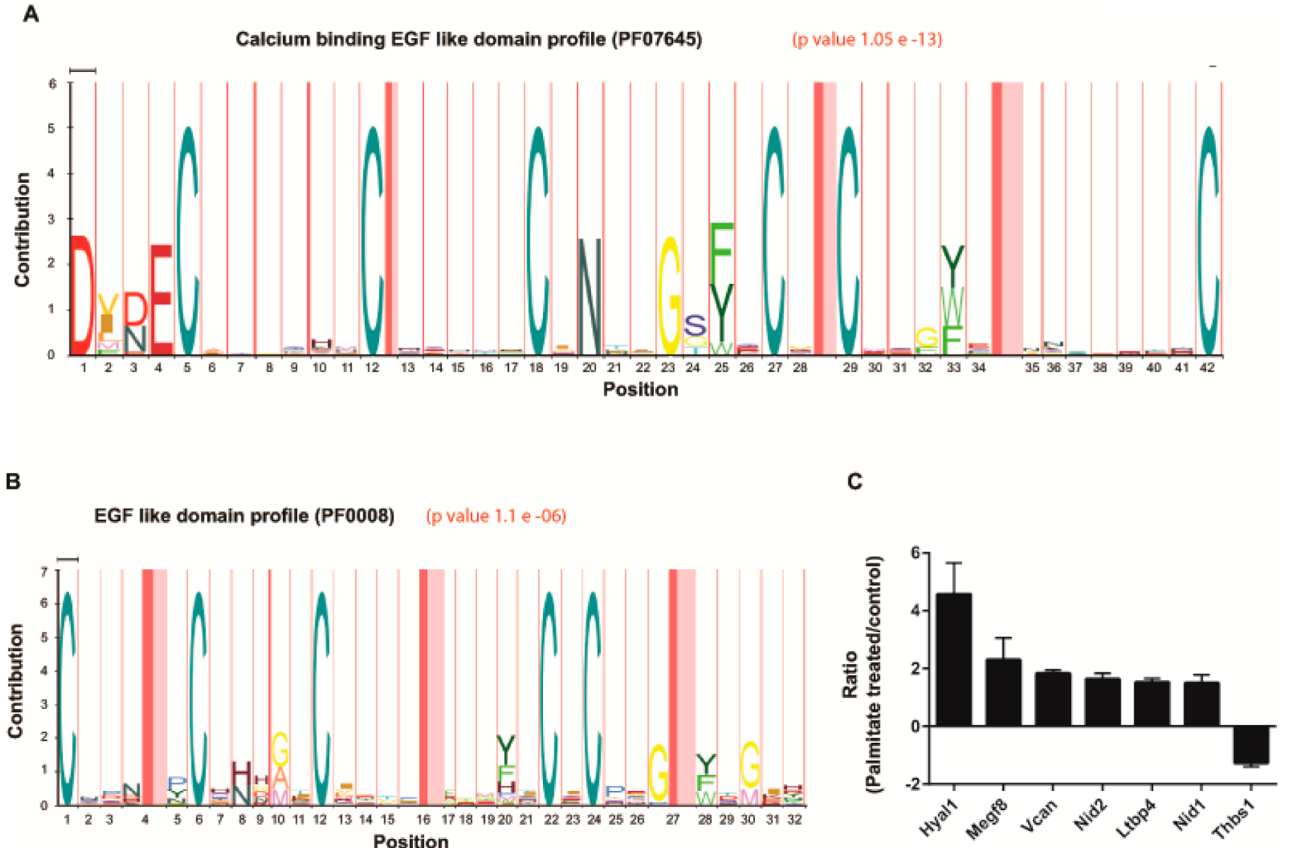

Figure 4. Secreted proteins regulated under palmitate-treated insulin-resistant conditions are enriched for EGF-like domain. (A,B) Enrichment of calcium-binding EGF domain (A) and EGF-like domain (B) after Fischer's exact test. (C) Abundance of few classically secreted proteins with EGF-like domain. Secretion of these proteins is induced under palmitate-treated insulin resistance conditions in skeletal muscle cells. Error bars are standard deviation from median.

Figure 2A). Thus, using this filtering strategy, our workflow led to the identification of 1073 putative secreted proteins from skeletal muscle cells (Figure 2A, Supplemental Table 2).

This list of proteins was strongly enriched for proteins annotated to be glycoprotein, signal-peptide-containing, and extracellular, whereas the number of proteins with intracellular annotation was substantially decreased (Figure 2A, total identified versus total secreted). Interestingly, 40% of these putative secreted proteins still had annotated intracellular locations in GOCC. Our bioinformatics workflow classifies these proteins as secreted because they either contained a predicted signal peptide (400 proteins) or were annotated to "extracellular locations" (GOCC) (44 proteins). Of the 400 proteins, 214 were assigned to "endoplasmic reticulum" (104) and or to "golgi" (53) or "membrane" (138). While we cannot be sure that this set of proteins is truly secreted, they contain known secreted proteins such as Bdnf, Anxa2, Bmp1, Mmp2, and apolipoprotein E. Our results further support the concept of multitasking proteins or "protein moonlighting".[12] Within the group of proteins, which we categorized as nonsecreted, a plurality (40%) was annotated to intracellular locations in GOCC (Supplemental Table 4). We cannot exclude the possibility that some of these proteins are true secreted proteins, that is, secretion via exosomes and microvesicles.

The presence of a high number of proteins with the "intracellular location" (GOCC) might be attributed to serum-deprivation and or palmitate-induced apoptosis of cells. To investigate whether our bioinformatics workflow separates these contaminating proteins from true secreted proteins, we correlated the proteins detected in the media and the cellular proteome of exactly the same samples. 90% of the proteins detected in media were also detected in cellular proteome. When we compared the intensities of proteins from the media and cell lysate, we observed a moderate correlation (R^2 = 0.37), suggesting that few abundant cellular proteins may have been released due to cell death (Figure S1C). Importantly, protein abundances were significantly different (Mann–Whitney p value = 0.028) in the conditioned media than in the cellular proteome (Figure 2B,C). Finally, despite presenting "myokinome", one should not undermine the limitations of computations tools and our incomplete knowledge of secretion biology. Additional experiments should be performed to verify candidates in secretome maps.

Comparative Secretome Analysis between Control and Insulin-Resistant C2C12 Cells

Although the pathophysiology of insulin resistance is still incompletely understood, it is believed that increased plasma levels of FFA and pro-inflammatory proteins are responsible for at least part of reduced insulin signaling and glucose utilization.[19,25,26] Additionally, it has been established that insulin signaling is impaired in human and animal models subjected to lipid infusion[21,25] and in skeletal muscle cells treated with FFAs such as palmitic acid.[20,22] Likewise, we showed that lipid treatment impaired insulin signaling in our cellular model (Figure 1B). Together, this suggests that it would be informative to compare the skeletal muscle secretome

DOI: 10.1021/acs.jproteome.5b00720
J. Proteome Res. 2015, 14, 4885−4895

of insulin-resistant skeletal muscle cells with the control. Using MaxQuant built-in label free-quantification algorithm,[34] we quantified ~3000 proteins in the conditioned media from each replicate (Figure 3A). We required stringent criteria for quantified proteins, considering only those that were quantified three or more times in at least the control or palmitate-treated group. As displayed in Figure 3A (red stacked graph), ~23% of the quantified proteins fell into the group of putative secreted proteins as previously determined. We examined the reproducibility within the biological quintuplicates and found very high correlations within the control and palmitate-treated groups (Pearson correlation = 0.97 and 0.96, respectively, Figure S2A,B). Median unique peptide numbers and sequence coverage for quantified secreted proteins were 9 and 33.2%, respectively. Figure S2C illustrates MSMS spectra of a peptide for Bdnf, the growth factor previously discussed.

To investigate whether our secretome analysis can segregate control and palmitate-treated insulin-resistant cells, we performed principal component analysis (PCA) (Figure 3B). Component 1 of the PCA accounted for 40% of total variance (horizontal axis in Figure 3B) and clearly separated the control group from palmitate-treated group. This demonstrates that media from the control and palmitate-treated insulin-resistant cells have protein secretion patterns that are sufficiently distinct to classify them as distinct entities. Examples of putative secreted proteins that drive the separation of control and palmitate-treated insulin-resistant conditions are indicated in the "PCA loadings" (Figure 3C). They include insulin-like growth factor binding protein 7 (Igfbp7) whose secretion is significantly down-regulated ($P < 9.8 \times 10^{-5}$) under the insulin-resistant conditions. Interestingly, a low plasma level of Igfbp7 is correlated with the incidence of type 2 diabetes in humans.[43] Secretory leucocyte protease inhibitor (Slpi) also helps to discriminate control and palmitate-treated secretomes (Figure 3C), and our measurements indicated 2 times higher levels in palmitate-treated insulin-resistant cells. Slpi is an anti-inflammatory protein whose expression is induced by high-fat diet in rodents.[44] We examined whether a specific group of proteins distinguishes palmitate-treated insulin-resistant secretomes from control, which identified the category "Signal" (UniProt Keyword, 555 proteins) as the topmost enriched category in the palmitate-treated state ($P < 3.9 \times 10^{-109}$, Figure 3D). These findings clearly imply that classical secreted proteins rather than contaminating intracellular proteins are responsible for the separation of control and palmitate treated groups.

To gain more insights into biological differences between secretomes of control and palmitate-treated insulin-resistant muscle cells, we performed two-sample *t* test (Figure 3E). This identified 378 significantly different putative secreted proteins (Figure 3E, Supplemental Table 3). The list of significantly different proteins obtained by unbiased proteomic analysis contains several proteins including pro-inflammatory cytokines and proteins from insulin-like growth factors (IGF) pathways, whose expression levels has already been described to be regulated under diabetes and or obesity. (See details later.) This encouraged us to further investigate properties of the regulated and putative secreted proteins. To check for specific domain structures or patterns in comparison with all identified proteins, we imported domain information from the Pfam database and performed Fischer's exact test with an FDR = 0.02. Among the domains with significant *p* value, the "calcium-binding EGF domain" and "EGF-like domain" were the topmost significant ($P < 1.05 \times 10^{-13}$, 1.1×10^{-6}, respectively) (Figure 4A,B). A few examples of classically secreted proteins with EGF-like domains, whose secretion was regulated under palmitate-treated insulin-resistant state, are shown in Figure 4C. None of these proteins were previously described in the context of skeletal muscle insulin resistance. Further studies are required to dissect the functional roles of these EGF domain-containing secreted proteins in skeletal muscle biology and insulin resistance.

Reduced Secretion of IGF and IGFBP under Palmitate-Treated Insulin-Resistant Conditions

Insulin-like growth factor 1 (Igf-1) is a multipotent growth factor with important activities in regulating growth and metabolism. Additionally, because of its glucose-lowering and insulin-sensitizing actions, it has beneficial effects on glucose homeostasis.[45] The abundance of Igf-1 was 3 times lower in the media from palmitate-treated cells compared with control cells, while levels of Igf-2 were similar (Figure 5A, Supplemental Table 2). This may be mediated by palmitic-acid-induced increase in TNF-a production,[46] which, in turn, decreases circulating levels of Igf-1.[47]

IGF binding proteins (IGFBPs) represent an important link between the insulin and IGF systems, and several lines of evidence suggest the strong association of different IGFBPs with type 2 diabetes.[45] In our experimental model, we successfully quantified Igfbp2, Igfbp4, and Igfbp5−7 and

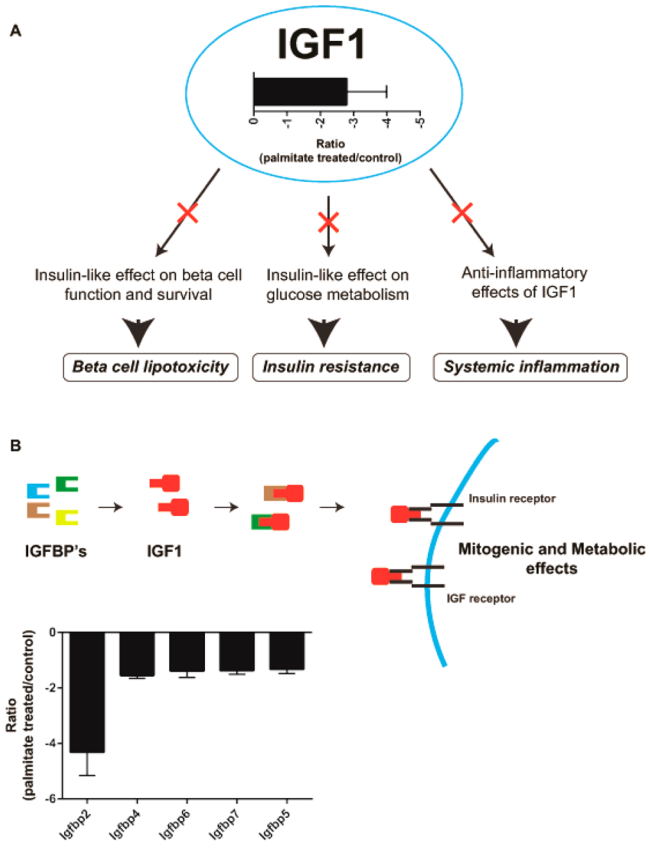

Figure 5. Reduced secretion of IGF and IGFBP under palmitate-treated insulin-resistant conditions. (A,B) Abundances of IGF-1 and IGFBP's in conditioned media from control and palmitate-treated insulin-resistant muscle cells. In panel B, error bars are standard deviation from median.

DOI: 10.1021/acs.jproteome.5b00720
J. Proteome Res. 2015, 14, 4885−4895

found that they all are downregulated under insulin resistance (Figure 5B).

Regulation of Cytokines and Chemokines

Pro-inflammatory cytokines and chemokines play an important role in the pathogenesis of type 2 diabetes and obesity.[6,48] An excess of nutrient causes aberrant release of adipokine, cytokine, and chemokine from adipose tissues, which leads to low-grade chronic inflammation, a hallmark feature of obesity.[48] Our data set contains 21 quantified proteins with known cytokine activity (Supplemental Table 5), 8 of which were significantly regulated under palmitate-treated insulin-resistant conditions (Figure 6). Serum levels of chemokines including

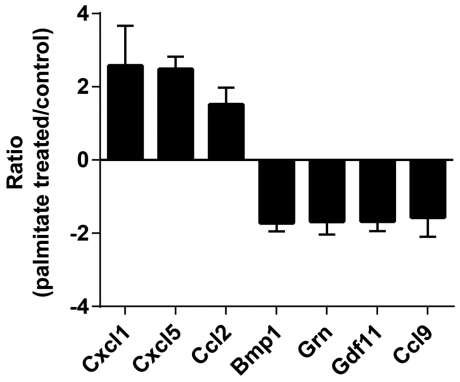

Figure 6. Quantification of regulated cytokines. Abundances of significantly regulated chemokines and cytokines in the media from control and palmitate-treated insulin-resistant cells. Error bars are standard deviation from median.

Ccl2, Ccl5, Ccl7, Ccl8, Ccl11, Ccl13, Cxcl1, Cxcl5, Cxcl8, and Cxcl10 are dramatically increased in obese versus lean individuals.[6,48] A majority of these chemokines were quantified in our study (Supplemental Table 5), and we confirmed that secretion of Cxcl1, Cxcl5, and Ccl2 chemokines was significantly increased in palmitate-treated insulin-resistant muscle cells ($P < 0.001$, 6.7×10^{-5}, 0.005, respectively) (Figure 6). Thus, in addition to adipose tissues, lipid-induced secretion of pro-inflammatory chemokines from skeletal muscle might contribute to the low-grade chronic inflammation.

Secretion of Granulin (Grn), growth/differentiation factor 11 (Gdf11), and bone morphogenetic protein 1 (Bmp1) were significantly decreased in palmitate-treated muscle cells ($P < 0.001$, 0.002, 1.2×10^{-5}, respectively) (Figure 6). Granulin (also known as progranulin) is a pleiotropic molecule regulating cell growth and anti-inflammatory functions.[49] Reduced secretion of granulin in combination with increased secretion of pro-inflammatory chemokines might exacerbate inflammatory response under insulin resistant conditions. Gdf11, which was recently reported to be a rejuvenating factor for skeletal muscle,[50] and, interestingly, it was significantly reduced in palmitate-treated insulin-resistant skeletal muscle ($P < 0.002$). Finally, secretion of Bmp1, which is known to regulate muscle cell growth by activation of latent myostatin,[51] was also reduced in palmitate-treated insulin-resistant muscle cells. Our findings suggest follow-up experiments to dissect the roles of circulating Gdf11 and Bmp1 in insulin-resistant conditions.

CONCLUSIONS

Here we have shown that a combination of large-scale quantitative proteomics and a streamlined bioinformatics workflow is a promising tool to study secretomes of skeletal muscles. We demonstrated how bioinformatics filter strategies can be applied to discriminate secretory proteins from those that likely originate from cell leakage. To our knowledge, this is the deepest, high-accuracy, quantitative secretome study on skeletal muscle to date. The approach described here could now be applied to study secretomes of other cellular models. Our data revealed significant differences in the secretomes of muscle cells as they become insulin-resistant. PCA analysis showed that these differences are mainly due to differential secretion of classical secreted proteins and not contaminating intracellular proteins. The significant quantitive differences between the secretomes of the control and palmitate-treated insulin-resistant muscle cells confirmed known markers previously discovered in other cellular, rodent, or human models of diabetes and highlighted novel ones, which include an interesting family of proteins containing signal peptide and EFF-like domain structure. Finally, our finding that secretion of IGF and IGF binding proteins was down-regulated under palmitate-treated insulin-resistant conditions suggests interesting avenues for follow up.

Our quantitative analyses of muscle secretomes provide a comprehensive resource to explore muscle biology and muscle-dependent cross talk with other tissues. The myokines defined in this study comprises about 1000 proteins; however, their function and regulation in context of muscle physiology is unexplored. We envision that skeletal-muscle-derived secreted proteins could vary under various environmental conditions. Therefore, further studies are required to clarify their regulation and their roles in distinct signaling pathways to understand their biological functions.

ASSOCIATED CONTENT

Supporting Information

The Supporting Information is available free of charge on the ACS Publications website at DOI: 10.1021/acs.jproteome.5b00720. The mass spectrometry proteomics data have been deposited to the ProteomeXchange Consortium (http://proteomecentral.proteomexchange.org) via the PRIDE partner repository with the dataset identifier PXD000288. The data can be accessed using the following information: ProteomeXchange submission title: Secretome of insulin resistant C2C12 cells. ProteomeXchange accession: PXD000288. PX reviewer account: Username: review39802, Password: krkYtJSw.

Figure S1. Comparison with published literature. Figure S2. Reproducibility of proteomic data. (PDF)

Supplemental Table 1. Table contains list of identified and quantified proteins in conditioned media from BSA (control) and palmitic acid (insulin resistance) treated cells. (XLSX)

Supplemental Table 2. List of the identified proteins that were enriched as secreted proteins. (XLSX)

Supplemental Table 3. List of significantly different proteins from control and palmitate-treated insulin resistant muscle cells after two-sample *t* test. (XLSX)

Supplemental Table 4. List of the quantified proteins that were predicted as "nonsecreted" by bioinformatics workflow. (XLSX)

DOI: 10.1021/acs.jproteome.5b00720
J. Proteome Res. 2015, 14, 4885−4895

Supplemental Table 5. List of identified and quantified cytokines. (XLSX)

AUTHOR INFORMATION

Corresponding Author

*Tel: 49-89-8578-2557. Fax: 49-89-8578-2219. E-mail: mmann@biochem.mpg.de.

Notes

The authors declare no competing financial interest.

ACKNOWLEDGMENTS

We thank Igor Paron and Korbinian Mayr for assistance in mass spectrometric analysis. We also thank Liu Jeffrey for critical reading of the manuscript. This work was supported by Federation of European Biochemical Societies (FEBS), Max-Planck Society for the Advancement of Science, and Novo Nordisk Foundation Center for Protein Research (NNF14CC0001)

ABBREVIATIONS

MS, mass spectrometry; FDR, false discovery rate; PCA, principal component analysis; GO, Gene Ontology; LFQ, label-free quantitation; FFA, free fatty acids; BSA, bovine serum albumin; PA, palmitic acid; EGF-like, epidermal growth factor-like; IGF, insulin-like growth factors; IGFBPs, insulin-like growth factors binding proteins; TNF-α, tumor necrosis factor alpha; IL-6, interleukin-6; IL-1b, interleukin 1beta; MCP-1, monocyte chemotactic proteins-1; NF-κB, nuclear factor κB; FBS, fetal bovine serum; Fgf21, fibroblast growth factor 21; Tgfb1, transforming growth factor beta; Bdnf, bone-derived neurotropic factor; Il34, interleukin 34; Ccl, chemokine (c-c motif) ligand; Cxcl, chemokine (c-x-c motif) ligand; ER, endoplasmic reticulum; Anxa, annexins; Hmgb, high mobility group protein b; Slpi, secretory leukocyte peptidase inhibitor; Grn, ganulins; Gdf11, growth/differentiation factor 11; Bmp1, bone morphogenic protein 1

REFERENCES

(1) DeFronzo, R. A.; Gunnarsson, R.; Bjorkman, O.; Olsson, M.; Wahren, J. Effects of insulin on peripheral and splanchnic glucose metabolism in noninsulin-dependent (type II) diabetes mellitus. *J. Clin. Invest.* **1985**, *76*, 149−55.

(2) DeFronzo, R. A.; Tripathy, D. Skeletal muscle insulin resistance is the primary defect in type 2 diabetes. *Diabetes Care* **2009**, *32* (Suppl 2), S157−63.

(3) Donath, M. Y. Targeting inflammation in the treatment of type 2 diabetes: time to start. *Nat. Rev. Drug Discovery* **2014**, *13*, 465−76.

(4) Feuerer, M.; Herrero, L.; Cipolletta, D.; Naaz, A.; Wong, J.; Nayer, A.; Lee, J.; Goldfine, A. B.; Benoist, C.; Shoelson, S.; Mathis, D. Lean, but not obese, fat is enriched for a unique population of regulatory T cells that affect metabolic parameters. *Nat. Med.* **2009**, *15*, 930−9.

(5) Vallerie, S. N.; Furuhashi, M.; Fucho, R.; Hotamisligil, G. S. A predominant role for parenchymal c-Jun amino terminal kinase (JNK) in the regulation of systemic insulin sensitivity. *PLoS One* **2008**, *3*, e3151.

(6) Yao, L.; Herlea-Pana, O.; Heuser-Baker, J.; Chen, Y.; Barlic-Dicen, J. Roles of the chemokine system in development of obesity, insulin resistance, and cardiovascular disease. *J. Immunol. Res.* **2014**, *2014*, 181450.

(7) Pedersen, B. K. The diseasome of physical inactivity–and the role of myokines in muscle–fat cross talk. *J. Physiol.* **2009**, *587*, 5559−68.

(8) Tuomilehto, J.; Lindstrom, J.; Eriksson, J. G.; Valle, T. T.; Hamalainen, H.; Ilanne-Parikka, P.; Keinanen-Kiukaanniemi, S.; Laakso, M.; Louheranta, A.; Rastas, M.; Salminen, V.; Uusitupa, M. Prevention of type 2 diabetes mellitus by changes in lifestyle among subjects with impaired glucose tolerance. *N. Engl. J. Med.* **2001**, *344*, 1343−50.

(9) Mann, M.; Kulak, N. A.; Nagaraj, N.; Cox, J. The coming age of complete, accurate, and ubiquitous proteomes. *Mol. Cell* **2013**, *49*, 583−90.

(10) Meissner, F.; Scheltema, R. A.; Mollenkopf, H. J.; Mann, M. Direct proteomic quantification of the secretome of activated immune cells. *Science* **2013**, *340*, 475−8.

(11) Caccia, D.; Dugo, M.; Callari, M.; Bongarzone, I. Bioinformatics tools for secretome analysis. *Biochim. Biophys. Acta, Proteins Proteomics* **2013**, *1834*, 2442−53.

(12) Huberts, D. H.; van der Klei, I. J. Moonlighting proteins: an intriguing mode of multitasking. *Biochim. Biophys. Acta, Mol. Cell Res.* **2010**, *1803*, 520−5.

(13) Yoon, J. H.; Kim, D.; Jang, J. H.; Ghim, J.; Park, S.; Song, P.; Kwon, Y.; Kim, J.; Hwang, D.; Bae, Y. S.; Suh, P. G.; Berggren, P. O.; Ryu, S. H. Proteomic analysis of the palmitate-induced myotube secretome reveals involvement of the annexin A1-FPR2 pathway in insulin resistance. *Mol. Cell. Proteomics* **2015**, *14*, 882.

(14) Yoon, J. H.; Song, P.; Jang, J. H.; Kim, D. K.; Choi, S.; Kim, J.; Ghim, J.; Kim, D.; Park, S.; Lee, H.; Kwak, D.; Yea, K.; Hwang, D.; Suh, P. G.; Ryu, S. H. Proteomic analysis of tumor necrosis factor-alpha (TNF-alpha)-induced L6 myotube secretome reveals novel TNF-alpha-dependent myokines in diabetic skeletal muscle. *J. Proteome Res.* **2011**, *10*, 5315−25.

(15) Yoon, J. H.; Yea, K.; Kim, J.; Choi, Y. S.; Park, S.; Lee, H.; Lee, C. S.; Suh, P. G.; Ryu, S. H. Comparative proteomic analysis of the insulin-induced L6 myotube secretome. *Proteomics* **2009**, *9*, 51−60.

(16) Hartwig, S.; Raschke, S.; Knebel, B.; Scheler, M.; Irmler, M.; Passlack, W.; Muller, S.; Hanisch, F. G.; Franz, T.; Li, X.; Dicken, H. D.; Eckardt, K.; Beckers, J.; de Angelis, M. H.; Weigert, C.; Haring, H. U.; Al-Hasani, H.; Ouwens, D. M.; Eckel, J.; Kotzka, J.; Lehr, S. Secretome profiling of primary human skeletal muscle cells. *Biochim. Biophys. Acta, Proteins Proteomics* **2014**, *1844*, 1011−7.

(17) Raschke, S.; Eckardt, K.; Bjorklund Holven, K.; Jensen, J.; Eckel, J. Identification and validation of novel contraction-regulated myokines released from primary human skeletal muscle cells. *PLoS One* **2013**, *8*, e62008.

(18) Henningsen, J.; Rigbolt, K. T.; Blagoev, B.; Pedersen, B. K.; Kratchmarova, I. Dynamics of the skeletal muscle secretome during myoblast differentiation. *Mol. Cell. Proteomics* **2010**, *9*, 2482−96.

(19) McGarry, J. D. Banting lecture 2001: dysregulation of fatty acid metabolism in the etiology of type 2 diabetes. *Diabetes* **2002**, *51*, 7−18.

(20) Schmitz-Peiffer, C.; Craig, D. L.; Biden, T. J. Ceramide generation is sufficient to account for the inhibition of the insulin-stimulated PKB pathway in C2C12 skeletal muscle cells pretreated with palmitate. *J. Biol. Chem.* **1999**, *274*, 24202−10.

(21) Yu, C.; Chen, Y.; Cline, G. W.; Zhang, D.; Zong, H.; Wang, Y.; Bergeron, R.; Kim, J. K.; Cushman, S. W.; Cooney, G. J.; Atcheson, B.; White, M. F.; Kraegen, E. W.; Shulman, G. I. Mechanism by which fatty acids inhibit insulin activation of insulin receptor substrate-1 (IRS-1)-associated phosphatidylinositol 3-kinase activity in muscle. *J. Biol. Chem.* **2002**, *277*, 50230−6.

(22) Powell, D. J.; Turban, S.; Gray, A.; Hajduch, E.; Hundal, H. S. Intracellular ceramide synthesis and protein kinase Czeta activation play an essential role in palmitate-induced insulin resistance in rat L6 skeletal muscle cells. *Biochem. J.* **2004**, *382*, 619−29.

(23) Hirabara, S. M.; Curi, R.; Maechler, P. Saturated fatty acid-induced insulin resistance is associated with mitochondrial dysfunction in skeletal muscle cells. *J. Cell. Physiol.* **2010**, *222*, 187−94.

(24) Chavez, J. A.; Summers, S. A. Characterizing the effects of saturated fatty acids on insulin signaling and ceramide and diacylglycerol accumulation in 3T3-L1 adipocytes and C2C12 myotubes. *Arch. Biochem. Biophys.* **2003**, *419*, 101−9.

(25) Brehm, A.; Krssak, M.; Schmid, A. I.; Nowotny, P.; Waldhausl, W.; Roden, M. Increased lipid availability impairs insulin-stimulated ATP synthesis in human skeletal muscle. *Diabetes* **2006**, *55*, 136−40.

DOI: 10.1021/acs.jproteome.5b00720
J. Proteome Res. 2015, 14, 4885−4895

(26) Wang, L.; Folsom, A. R.; Zheng, Z. J.; Pankow, J. S.; Eckfeldt, J. H. ARIC Study Investigators. Plasma fatty acid composition and incidence of diabetes in middle-aged adults: the Atherosclerosis Risk in Communities (ARIC) Study. *Am. J. Clin. Nutr.* **2003**, *78*, 91−8.
(27) Wisniewski, J. R.; Zougman, A.; Nagaraj, N.; Mann, M. Universal sample preparation method for proteome analysis. *Nat. Methods* **2009**, *6*, 359−62.
(28) Rappsilber, J.; Ishihama, Y.; Mann, M. Stop and go extraction tips for matrix-assisted laser desorption/ionization, nanoelectrospray, and LC/MS sample pretreatment in proteomics. *Anal. Chem.* **2003**, *75*, 663−70.
(29) Cox, J.; Neuhauser, N.; Michalski, A.; Scheltema, R. A.; Olsen, J. V.; Mann, M. Andromeda: a peptide search engine integrated into the MaxQuant environment. *J. Proteome Res.* **2011**, *10*, 1794−805.
(30) Scheltema, R. A.; Mann, M. SprayQc: a real-time LC-MS/MS quality monitoring system to maximize uptime using off the shelf components. *J. Proteome Res.* **2012**, *11*, 3458−66.
(31) Cox, J.; Mann, M. MaxQuant enables high peptide identification rates, individualized p.p.b.-range mass accuracies and proteome-wide protein quantification. *Nat. Biotechnol.* **2008**, *26*, 1367−72.
(32) Petersen, T. N.; Brunak, S.; von Heijne, G.; Nielsen, H. SignalP 4.0: discriminating signal peptides from transmembrane regions. *Nat. Methods* **2011**, *8*, 785−6.
(33) Bendtsen, J. D.; Jensen, L. J.; Blom, N.; Von Heijne, G.; Brunak, S. Feature-based prediction of non-classical and leaderless protein secretion. *Protein Eng., Des. Sel.* **2004**, *17*, 349−56.
(34) Cox, J.; Hein, M. Y.; Luber, C. A.; Paron, I.; Nagaraj, N.; Mann, M. Accurate proteome-wide label-free quantification by delayed normalization and maximal peptide ratio extraction, termed MaxLFQ. *Mol. Cell. Proteomics* **2014**, *13*, 2513−26.
(35) Tusher, V. G.; Tibshirani, R.; Chu, G. Significance analysis of microarrays applied to the ionizing radiation response. *Proc. Natl. Acad. Sci. U. S. A.* **2001**, *98*, 5116−21.
(36) Ueki, K.; Yamamoto-Honda, R.; Kaburagi, Y.; Yamauchi, T.; Tobe, K.; Burgering, B. M.; Coffer, P. J.; Komuro, I.; Akanuma, Y.; Yazaki, Y.; Kadowaki, T. Potential role of protein kinase B in insulin-induced glucose transport, glycogen synthesis, and protein synthesis. *J. Biol. Chem.* **1998**, *273*, 5315−22.
(37) Nickel, W.; Rabouille, C. Mechanisms of regulated unconventional protein secretion. *Nat. Rev. Mol. Cell Biol.* **2009**, *10*, 148−55.
(38) Deshmukh, A. S.; Murgia, M.; Nagaraj, N.; Treebak, J. T.; Cox, J.; Mann, M. Deep proteomics of mouse skeletal muscle enables quantitation of protein isoforms, metabolic pathways and transcription factors. *Mol. Cell. Proteomics* **2015**, *14*, 841.
(39) de Azua, S. R.; Matute, C.; Stertz, L.; Mosquera, F.; Palomino, A.; de la Rosa, I.; Barbeito, S.; Vega, P.; Kapczinski, F.; Gonzalez-Pinto, A. Plasma brain-derived neurotrophic factor levels, learning capacity and cognition in patients with first episode psychosis. *BMC Psychiatry* **2013**, *13*, 27.
(40) Matthews, V. B.; Astrom, M. B.; Chan, M. H.; Bruce, C. R.; Krabbe, K. S.; Prelovsek, O.; Akerstrom, T.; Yfanti, C.; Broholm, C.; Mortensen, O. H.; Penkowa, M.; Hojman, P.; Zankari, A.; Watt, M. J.; Bruunsgaard, H.; Pedersen, B. K.; Febbraio, M. A. Brain-derived neurotrophic factor is produced by skeletal muscle cells in response to contraction and enhances fat oxidation via activation of AMP-activated protein kinase. *Diabetologia* **2009**, *52*, 1409−18.
(41) Gardella, S.; Andrei, C.; Ferrera, D.; Lotti, L. V.; Torrisi, M. R.; Bianchi, M. E.; Rubartelli, A. The nuclear protein HMGB1 is secreted by monocytes via a non-classical, vesicle-mediated secretory pathway. *EMBO Rep.* **2002**, *3*, 995−1001.
(42) Christmas, P.; Callaway, J.; Fallon, J.; Jones, J.; Haigler, H. T. Selective secretion of annexin 1, a protein without a signal sequence, by the human prostate gland. *Biochem. Soc. Trans.* **1991**, *266*, 2499−507.
(43) Gu, H. F.; Gu, T.; Hilding, A.; Zhu, Y.; Karvestedt, L.; Ostenson, C. G.; Lai, M.; Kutsukake, M.; Frystyk, J.; Tamura, K.; Brismar, K. Evaluation of IGFBP-7 DNA methylation changes and serum protein variation in Swedish subjects with and without type 2 diabetes. *Clin. Epigenet.* **2013**, *5*, 20.
(44) Adapala, V. J.; Buhman, K. K.; Ajuwon, K. M. Novel anti-inflammatory role of SLPI in adipose tissue and its regulation by high fat diet. *J. Inflammation (London, U. K.)* **2011**, *8*, 5.
(45) Rajpathak, S. N.; Gunter, M. J.; Wylie-Rosett, J.; Ho, G. Y.; Kaplan, R. C.; Muzumdar, R.; Rohan, T. E.; Strickler, H. D. The role of insulin-like growth factor-I and its binding proteins in glucose homeostasis and type 2 diabetes. *Diabetes/Metab. Res. Rev.* **2009**, *25*, 3−12.
(46) Jove, M.; Planavila, A.; Sanchez, R. M.; Merlos, M.; Laguna, J. C.; Vazquez-Carrera, M. Palmitate induces tumor necrosis factor-alpha expression in C2C12 skeletal muscle cells by a mechanism involving protein kinase C and nuclear factor-kappaB activation. *Endocrinology* **2006**, *147*, 552−61.
(47) Fan, J.; Char, D.; Bagby, G. J.; Gelato, M. C.; Lang, C. H. Regulation of insulin-like growth factor-I (IGF-I) and IGF-binding proteins by tumor necrosis factor. *Am. J. Physiol.* **1995**, *269*, R1204−12.
(48) Nunemaker, C. S.; Chung, H. G.; Verrilli, G. M.; Corbin, K. L.; Upadhye, A.; Sharma, P. R. Increased serum CXCL1 and CXCL5 are linked to obesity, hyperglycemia, and impaired islet function. *J. Endocrinol.* **2014**, *222*, 267−76.
(49) Kessenbrock, K.; Frohlich, L.; Sixt, M.; Lammermann, T.; Pfister, H.; Bateman, A.; Belaaouaj, A.; Ring, J.; Ollert, M.; Fassler, R.; Jenne, D. E. Proteinase 3 and neutrophil elastase enhance inflammation in mice by inactivating antiinflammatory progranulin. *J. Clin. Invest.* **2008**, *118*, 2438−47.
(50) Sinha, M.; Jang, Y. C.; Oh, J.; Khong, D.; Wu, E. Y.; Manohar, R.; Miller, C.; Regalado, S. G.; Loffredo, F. S.; Pancoast, J. R.; Hirshman, M. F.; Lebowitz, J.; Shadrach, J. L.; Cerletti, M.; Kim, M. J.; Serwold, T.; Goodyear, L. J.; Rosner, B.; Lee, R. T.; Wagers, A. J. Restoring systemic GDF11 levels reverses age-related dysfunction in mouse skeletal muscle. *Science* **2014**, *344*, 649−52.
(51) Wolfman, N. M.; McPherron, A. C.; Pappano, W. N.; Davies, M. V.; Song, K.; Tomkinson, K. N.; Wright, J. F.; Zhao, L.; Sebald, S. M.; Greenspan, D. S.; Lee, S. J. Activation of latent myostatin by the BMP-1/tolloid family of metalloproteinases. *Proc. Natl. Acad. Sci. U. S. A.* **2003**, *100*, 15842−6.

DOI: 10.1021/acs.jproteome.5b00720
J. Proteome Res. 2015, 14, 4885−4895